Control of MEMS Coriolis Vibratory Gyroscopes

Zurich Instruments

Application Note
Products: HF2PLL, HF2LI-MF, HF2LI-MOD

Release date: October 2015

Summary

This application note gives an overview of different control mechanisms for MEMS Coriolis Vibratory Gyroscopes (CVG) and how they are implemented using the commercial off-the-shelf HF2LI Lock-in Amplifier. A MEMS gyroscope is a micro-machined inertial device that can measure the angle of orientation or the angular rate of rotation. The principle relies on a vibrating structure that is suspended in a way that Coriolis forces can be sensed as the mass undergoes a rotation relative to the inertial space. These Coriolis forces can be efficiently sensed by means of lock-in amplifiers. Additionally, feedback control is usually employed to optimize the vibration properties and improve the overall performance. For highly accurate sensing, the control infrastructure can become complex and a number of control loops are running in parallel.

Practical implementations of open-loop and closed-loop control examples are presented in this document. It will be explained how to perform a basic gyroscope drive-mode control by means of a phase-locked loops (PLL) and automatic gain control (AGC). The drive-mode control is then combined with either open-loop sensing or closed-loop force-to-rebalance operation. Furthermore, we will explain electro-mechanical amplitude modulation. In this scheme all the signals of interest are amplitude modulated. This can improve the gyroscope performance by rejecting parasitic effects.

The HF2LI offers a variety of features, which makes it a powerful instrument for driving and characterizing vibratory gyroscopes, accelerometers and other MEMS oscillating structures. The key features are built-in signal modulation and demodulation at several frequencies in parallel, PLLs, amplitude control and PID controllers. Furthermore, the two 50 MHz low-noise signal input and output pairs allow for full control of both, the drive and the sense, modes of gyroscope vibration (see Figure 1).

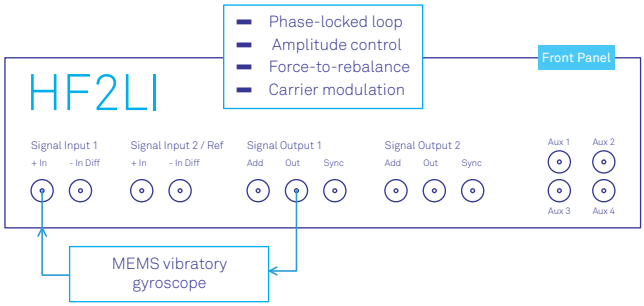

Figure 1. The Zurich Instruments HF2LI lock-in amplifier incorporates the infrastructure to perform basic resonator control as well as advanced gyroscope operation.

Theoretical Background

A gyroscope is an inertial device for measuring the angle of orientation or angular rate of rotation with respect to the inertial frame of reference. The most common MEMS gyroscope is the CVG which is a mass-spring-damper harmonic oscillator, which typically consists of a vibrating structure (proof-mass) with two degrees-of-freedom to allow unconstrained motion along both X and Y axes. The relative orientation between mounting platform and vibrating structure is measured to extract Coriolis acceleration, which contains the information about the applied rotation.

Gyroscopes are designed to be utilized in a wide range of rotation sensing applications, including defense, aviation, automotive and consumer markets, such as GPS navigation systems, smart phones and health-monitoring systems. They can be classified depending on their measurement type (Shkel 2006): (i) the angular rotation rate measurement (rate gyroscope), or (ii) the angle of rotation measurement (rate integrating or whole-angle gyroscope). Most of the commercial MEMS gyroscopes, are angular rate measuring sensors, and only few MEMS gyroscopes (Prikhodko 2011, Gregory 2012, Woo 2014, Trusov 2014) can be instrumented for direct angle measurements due to the stringent requirements on resonator stability, the sensor's mechanical structure and intricate control algorithms. Since the first demonstration of an electrostatically actuated tuning-fork gyroscope in Draper Lab (Bernstein 1993), variety of designs have been explored and published in open literature (Yazdi 1998, Xie 2003). However, the tuning-fork design is the leading gyroscope architecture in automotive industry commercialized by Robert Bosch GmbH and later by Analog Devices Inc. To date, ADI remains the pioneer in monolithic integrated MEMS gyroscopes (Greiff 1991, Prikhodko 2014), where mechanical elements of the gyroscope are integrated with circuits in one fabrication process.

Theory of operation of a CVG

The working principle of a CVG can be explained with a simplified lumped-element model as shown in Figure 2. The model is based on a proof-mass attached to the a frame by means of elastic springs, such that it can vibrate on the X-Y plane without constraints. The two possible orthogonal modes of vibration are usually referred to as drive-mode and sense-mode. The modes are coupled by the dynamics of the Coriolis force.

While the in-depth analysis of gyroscope dynamics is reported in (Lynch 1998), here we briefly discuss the main results in order to explain the modes of control. The CVG can be modeled as a harmonic oscillator with two degrees of freedom (drive-mode and sense-mode). A simplified set of differential equations for the motion of vibrating mass in the rotating frame of reference (non-inertial frame) is given by:

$$Mx'' + D_x x' + K_x x = f_x + 2M\Omega \cdot y' \quad (1)$$

$$My'' + D_y y' + K_y y = f_y - 2M\Omega \cdot x' \quad (2)$$

where x and y are the displacements of the drive- and sense-mode motions, D_x and D_y are the damping coefficients of the drive- and sense-mode, K_x and K_y are the spring constants, corresponding to the stiffness of the drive- and sense-mode, f_x and f_y are the forces applied to the gyroscope drive- and sense-modes, respectively, M is the mass of the gyroscope proof-mass, Ω is the input rotation rate around z-axis. The terms $2M\Omega \cdot y'$ and $2M\Omega \cdot x'$ represent the Coriolis force coupling the two modes of vibration.

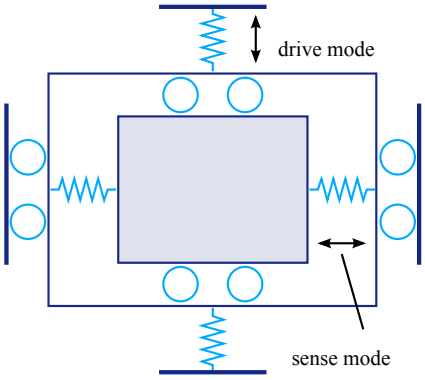

Figure 2. Two-dimensional model of a CVG. The proof mass M can oscillate freely in the x and y direction, also called drive and sense mode direction. Upon rotation around the z axis the oscillation in the x direction will lead to an oscillation in the y direction due to the Coriolis force.

Usually, the drive force f_x in the form $f_x = f_{xs}\sin(\omega_x t)$ is used to excite and sustain the oscillations at resonance $\omega_x = \sqrt{K_x/M}$, f_{xs} is the magnitude of the applied force. By employing both amplitude control and a phase-locked loop, a constant amplitude c_{x0} results, such that $x = c_{x0}\cos(\omega_x t)$.

Substituting these equations into Equation 2, we obtain

$$My'' + D_y y' + K_y y = f_y + 2M\Omega \cdot c_{x0}\omega_x \sin(\omega_x t) \quad (3)$$

to show that upon rotation the Coriolis force leads to an amplitude modulated vibration in the sense mode (y-axis) at the same frequency.

The sense-mode can be operated in open-loop or closed loop. In open-loop, the force f_y is zero ($f_y = 0$) and the solution is

$$y = -c_{x0}\tau_y\Omega \cdot \cos(\omega_x t) \quad (4)$$

where τy is the amplitude-decay time constant given by (for ideal case when $\omega_x = \omega_y$):

$$\tau_y = 2Q_y/\omega_y \quad (5)$$

Here, $Q_y = \omega_y \cdot M/D_y = \tau_y\omega_y/2$ and $\omega_y = \sqrt{K_y/M}$ are the quality factor and the resonance frequency of the sense-mode.

In other words, the sense-mode displacement y is a direct measure of the applied angular rate Ω. More specifically, the amplitude of the oscillation along the y-axis can be measured by means of a lock-in amplifier measuring amplitude at frequency ω_x.

In order to increase the bandwidth and dynamic range of the MEMS gyroscope, closed-loop control of the sense mode is often employed. In the so-called force-to-rebalance (closed loop) mode, a feedback force is generated to suppress the sense-mode motion. In this case, the force f_y in the form $f_y = f_{ys}\sin(\omega_x t)$ is used to maintain y at zero. The magnitude f_{ys} of the applied force f_y is a direct measure of the input angular rate Ω. In order to also compensate for the quadrature term (arising from the frequency mismatch $\Delta\omega = \omega_x - \omega_y$ and the misalignment of the proof-mass), the applied force f_y should be in the form:

$$f_y = f_{ys}\sin(\omega_x t) + f_{yc}\cos(\omega_x t) \quad (6)$$

where the multiple f_{ys} of the sine term is used to drive the Coriolis signal to zero, and the multiple f_{yc} of the cosine term is used to drive the quadrature signal to zero.

In this document, we will use a compact notation of slow varying components c_x, s_x, c_y, s_y as used in (Lynch 1998, Leland 2005). They can be defined by performing a coordinate transformation in the form:

$$x = c_x\cos(\omega_x t) + s_x\sin(\omega_x t) \quad (7)$$

$$y = c_y\cos(\omega_x t) + s_y\sin(\omega_x t) \quad (8)$$

The variables c_x and s_x represent the demodulated components of the drive-mode motion x. Similarly, c_y and s_y represent the demodulated components of the sense-mode motion y. The physical meaning of these components is the following: c_x represents the drive-mode amplitude, s_x represents the drive-mode phase, c_y represents the Coriolis amplitude (proportional to the rotation rate), and s_y represents the quadrature error.

Overview of the HF2LI Lock-in Amplifier

In order to understand how the HF2LI digital lock-in amplifier is used for gyroscope applications, it is helpful to explain the internal structure of the instrument.

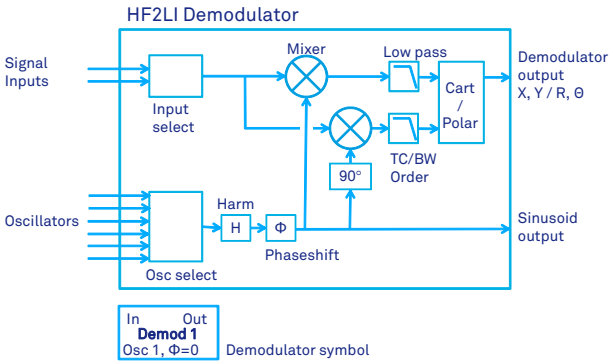

Figure 3. HF2LI demodulator schematic with the different settings, which are summarized in Table 1. The simplified symbol at the bottom is used in the schematics of this document.

The most essential component of every lock-in amplifier is the demodulator which performs a very narrow-band filtering of the signal of interest around a determined frequency. The result of the demodulation is a precise measurement of the amplitude and the phase of the signal even when the signal is seemingly covered by noise. The essential structures of the HF2LI demodulator are shown in Figure 3. The demodulator comprises a signal input selector, an oscillator input selector, two mixers, two low-pass filters and a cartesian-to-polar converter. The selected input signal is multiplied by the normalized sine coming from one of the six input oscillators, which runs at a defined frequency ω. The sine may be a harmonic of ω and it may be phase shifted before applied to the mixers. Two mixers, with 90° phase shift against each other, are employed to determine the in-phase and out-of-phase components of the input signal, and, thereby allowing to calculate the amplitude and the phase of the input signal at frequency ω. The modulator output, as depicted in the diagram, is affected by the harmonic and phase shift settings and can be used as an excitation signal to the setup.

A summary of all settings of the HF2LI demodulator is given in Table 1.

Table 1. Demodulator parameters

Signal / parameter	Description
Input select	Each demodulator can be connected to either of the two signal inputs
Osc select	Each demodulator can be connected to any of the six oscillators.

Table 1. Demodulator parameters

Signal / parameter	Description
Harm	Harmonic, usually "1". Frequency multiplication to demodulate higher harmonics.
Phase shift ?	Phaseshift between oscillator and input/output mixer
TC, BW	Time constant or bandwidth of the low pass filter
Order	Filter order from 1 to 8
Demodulator output	X, Y, R, Θ of the measured signal
Sinusoid output	Sinusoid signal that can be connected to any of the two signal outputs

As shown in Figure 4, the HF2LI comprises 8 dual-phase demodulators, two of them are used for PLL operations and six of them can be configured by the user in the most flexible way. Input and output mixers allow to basically connect any demodulator input or output to any of the two physical input and outputs of the device. The output multiplexers can amplify and add up the signals from the different demodulators. This allows to digitally combine the signals from two or more modulator outputs.

Furthermore, the HF2LI offers a modulation option (HF2LI-MOD), which allows performing amplitude or frequency modulation and demodulation. With the modulation option, the oscillators driving the demodulator of Figure 3 can be changed such that the demodulator performs an amplitude demodulation. As shown in Figure 5, the oscillator signals applied to the demodulator 2 and 3 are now the sum and difference of the two frequencies.

As a consequence, it is possible to perform direct sideband demodulation of an amplitude modulated signal. For example, a signal with carrier frequency of f_1=52 kHz and an amplitude modulation frequency of f_2=f_3=2 kHz can be directly demodulated at the sideband frequencies 52+2 kHz and 52-2 kHz. Traditionally, two lock-in amplifiers in series were required to perform this operation. Furthermore, in the HF2LI, one or both of the modulation and the carrier frequency can be either fixed or also controlled by a PLL. This allows for performing direct sideband demodulation, while, at the same time, running the resonator at its natural resonance frequency by means of a PLL.

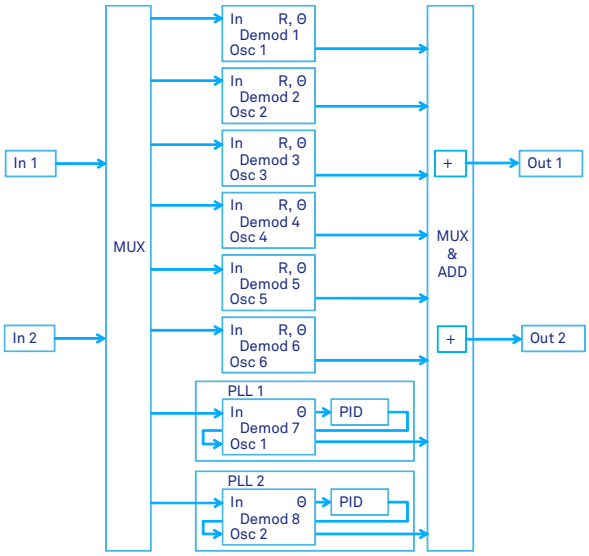

Figure 4. HF2LI input and output schematic showing 2 signal inputs, 2 signal generator outputs, 6 dual-phase demodulators and 2 phase-locked loops (shown schematic requires both HF2LI-PLL and HF2LI-MF option).

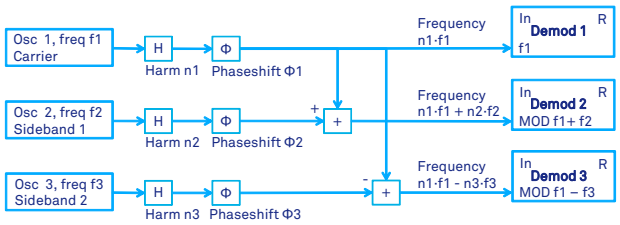

Figure 5. Schematic of three of the HF2LI demodulators with amplitude modulation applied. With the modulation option of the HF2LI, the user can define the carrier frequency f1 and the sideband frequencies f2 and f3 of the amplitude modulation. As a consequence, the demodulator 2 will run at the sum frequency f1+f2 and the demodulator 3 at the difference frequency f1-f2 (if no harmonics are used). This allows to directly demodulate the signal at the sidebands f1+f2 and f1-f2. Any of the oscillator frequencies f1, f2 and f3 can be dynamic, thereby, e.g., controlled by a PLL or an external reference.

Gyroscope Operation

In this section, we will discuss the most important control and sensing modes for MEMS gyroscopes using the HF2LI lock-in amplifier. It should help the reader to understand the basics of gyroscope control mechanisms as well as how to use the HF2LI lock-in amplifier for both control of drive- and sense-modes of vibration.

Drive mode control

For the drive-mode control, the oscillation of the vibratory gyroscope is maintained at resonance by means of a PLL. Furthermore, the mechanical amplitude is kept constant using a PID controller; otherwise temperature drift may degrade the performance of the CVG.

The basic setup is described in Figure 6. The drive-mode of the gyroscope is connected to input and output of the HF2LI. It is important to note that there may be additional circuitry required, which is not shown, e.g., current-to-voltage conversion. For electrostatic actuation, an offset (V_{Offset}) is often applied to the drive signal. This offset can be added with external circuitry or, very conveniently, by using the Add connector on the HF2LI front panel. The PLL locks to the resonance frequency of the drive mode. For the excitation of the drive-mode, the modulator output of Demodulator 1 is used. The phase shift Φ_X of the modulator is set to maximize the amplitude of oscillations. The phase Φ_X is typically 90 degrees unless the gyroscope's electronics is adversely affecting the signal phases. This closes the PLL loop as the frequency of oscillator 1 is controlled by the PLL 1. In addition, an AGC loop keeps the excitation amplitude constant. The AGC uses a PID controller to compare and regulate the drive mode oscillation amplitude to a given setpoint. The demodulator output X (c_x from Equation 7) of the Demodulator 2 with zero phase shift serves as an input to the PID controller. Note, the second demodulator is required to set the demodulation phase independently of the modulator output phase (see Figure 3 for details).

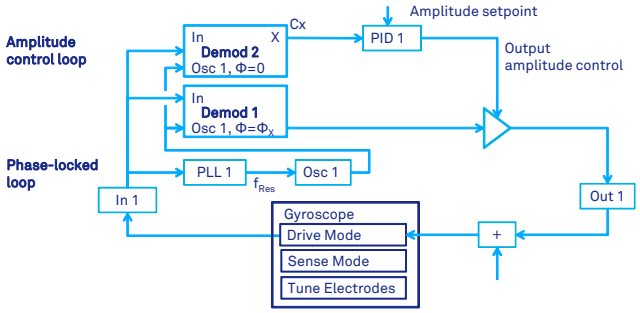

Figure 6. Gyroscope or general resonator drive-mode control by means of a phase-locked loop and a PID controller for automatic gain control. The PLL keeps the resonator at its natural resonance frequency. The PID keeps fixed resonator amplitude.

Sense mode open-loop control

In the simplest gyroscope instrumentation, the gyroscope drive-mode control is applied as described in the previous section, while the sense-mode is implemented in open loop. This scheme is one of the basic operation principles and is widely used, one example can be found in (Prikhodko 2012) and in (Prikhodko 2013). As shown in Figure 7, the input of Demodulator 3 is connected to the gyroscope sense-mode output. Demodulator 3 uses Oscillator 1, which is controlled by the PLL. The demodulator phase shift Φ_Y is adjusted to ensure the component Y of Demodulator 3 is the Coriolis output (c_y in Equation 8) proportional to the angular rate, and the component X of Demodulator 3 is the quadrature error (s_y in Equation 8). The phase Φ_Y is typically set by trial and error until component X is not sensitive to rotation (when gyroscope is rotating). It could vary from -90 degree to 90 degrees depending on the mode-matching condition (difference between the drive- and sense-mode natural frequencies). The gyroscope response time to the input rotation is limited by the amplitude-decay time constant τ_y (Equation 5), which, in turn, limits the gyroscope bandwidth (Lynch 1998). In order to increase the bandwidth (reduce the response time) and eliminate the effect of the frequency mismatch $\Delta\omega$ on the gyroscope scale-factor, the force-to-rebalance control must be employed (see next Section).

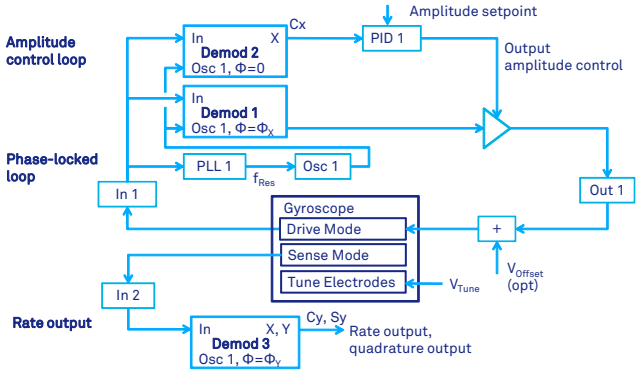

Figure 7. Gyroscope control with closed-loop drive-mode and open-loop sense-mode measurement. The drive mode is controlled by means of a PLL and an AGC. The gyroscope output is an oscillation in the sense mode which is measured by a demodulator running at the same frequency as the PLL of the drive-mode.

Force-to-rebalance control

The force-to-rebalance (FTR) mode of operation for rate measuring gyroscope is described in details in (Lynch 1998). Figure 8 shows four control loops for drive- and sense-modes of a MEMS Coriolis Vibratory Gyroscope. Specifically, two input signals from the gyroscope (from drive and sense mode) are demodulated to obtain in-phase and in-quadrature (out-of-phase) signals s_x, c_x, s_y, c_y (notations are conveniently adopted from (Lynch 1998), see Equation 7 and Equation 8). The signals s_x and c_x are the in-phase X and out-of-phase Y components of the demodulator outputs of the drive-mode vibration, respectively, see Equation 7. Likewise, the signals c_y and s_y are the in-phase X and out-of-phase Y components of the sense-mode demodulator. When demodulation phases Φ_X and Φ_Y are set as explained in previous sections, the physical meaning of these signals is the following: c_x represents the drive-mode amplitude, s_x represents the drive-mode phase, c_y represents the Coriolis amplitude (proportional to the rotation rate), and s_y represents the quadrature error.

These four signals serve as an input for the four control loops, one of which is a PLL. Although PID controllers are employed, the differential term D is usually not used. The

control signals from the PID loops add up to obtain one drive output, which is fed back to the gyroscope for sense-mode control. The drive-mode control is the same as explained in the previous section. The PID controller 2 maintains the output Y of Demodulator 3 (c_y in Equation 8) at zero by regulating an amplitude of the modulator Output 2 from Demodulator 4 (with 90 degrees phase shift). Similarly, PID controller 3 maintains the output X of Demodulator 3 (s_y in Equation 8) at zero by regulating an amplitude of the modulator Output 2 from Demodulator 2 (with 0 degree phase shift).

The FTR mode extends the bandwidth of the gyroscope beyond the limitation of the open-loop sense-mode, which is usually limited by the amplitude decay time constant. The FTR loop bandwidth is controlled by the P and I gains. In addition, the FTR scale-factor is more stable since it doesn't depend on the frequency mismatch (in contrast to the open-loop scale-factor).

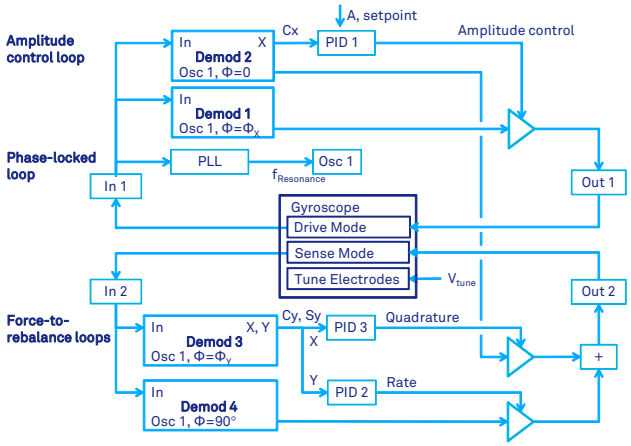

Figure 8. Gyroscope control with both closed-loop drive-mode and closed loop sense-mode. This mode is usually called force-to rebalance (FTR). With FTR, the rate and quadrature output of the sense mode are suppressed by means of feedback control. The necessary feedback force is a measure of the rate of angular rotation.

Carrier modulation

For gyroscope applications, the detection sensitivity is enhanced by using a carrier frequency modulation scheme (Trusov 2007). Carrier modulation rejects the background noise and contributions from parasitic effects. The HF2LI is a particularly well suited instrument for this purpose, as it is the only digital lock-in amplifier with sufficient infrastructure in a single device for a complete control of drive and sense mode including carrier modulation.

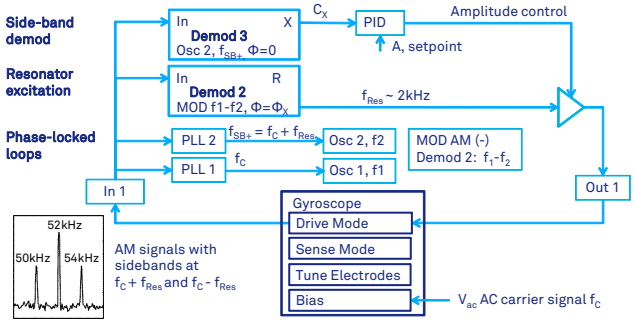

Figure 9. Gyroscope drive-mode control when the carrier modulation is employed. The gyroscope signal at resonance frequency fRes is amplitude modulated with carrier frequency fc. As a result, the signal of interest is shifted to the frequencies fc+fRes and fc-fRes. The shown setup (i) locks to the sideband fc+fRes by means of a PLL, (ii) demodulates directly the sideband at fc+fRes, (iii) computes the excitation frequency fRes from fc+fRes and fc by means of the MOD option, and (iv) excites the gyroscope drive mode at fRes with gain control (AGC).

In addition to the previously presented control loops, a carrier signal at frequency f_C (an order of magnitude higher than the gyroscope resonant motion) is employed for separation from parasitic-capacitance feed through. The demodulator in this case operates as shown in Figure 9. This technique is employed in, e.g., (Prikhodko 2011, Prikhodko 2012) and is referred to as Electromechanical Amplitude Modulation (EAM). Its implementation requires side-band demodulation of gyroscope motion signals in both drive and sense directions, which in case of the quadruple-mass gyroscope (QMG) used in (Prikhodko 2011) is typically at 2 kHz modulation frequency and the carrier signal is chosen at 52 kHz.

As shown in Figure 9, Figure 10 and Figure 11, the 52 kHz carrier signal from a signal generator is fed to the gyro ground. The first lock-in amplifier input is used for drive-mode signal pick-off from the gyroscope, and the second input is for sense-mode signal read-out. While the first output is used for the drive-mode control, the second output is reserved to control the sense-mode, both generating output signals around the natural oscillation frequency of the gyroscope, which is in this case around 2 kHz.

As described in previous section, the closed-loop gyroscope operation requires simultaneous control of three variables: c_x (amplitude), c_y (rate) and s_y (quadrature). This is accomplished by three PID controllers (excluding the PLL) and three modulators producing feedback signals at the frequency of Oscillator 1 and having three different phase shifts relative to each other. The amplitude of the drive-mode oscillation is measured by the Demodulator 3 and controlled by the PID 1. The rate and quadrature of the sense-mode oscillation are measured by the Demodulator 6 and controlled by the PID 2 and PID 3 respectively. If the demodulation phases for Demodulators 3 and 6 are set to zero and Φ_Y (explained in the pre-

vious section), the component X of Demodulator 3 is amplitude, the component Y of Demodulator 6 is rate, and the component X of Demodulator 6 is quadrature. These three demodulated components are fed to PIDs, which sustain the amplitude at a constant level, the rate signal at zero, and the quadrature also at zero. To form a feedback signal the outputs of PID outputs are modulated (i.e. by controlling the output amplitude of the oscillator signals). Assuming negligible phase shifts in gyroscope's front-end electronics, the modulator output of Demodulator 2 with 90 degree phase shift is used for both amplitude and rate feedback. While the modulator output of Demodulator 5 with 0 degree phase shift is used for quadrature nulling. Finally, before feeding back the control signal to the gyroscope, the modulated outputs are summed up.

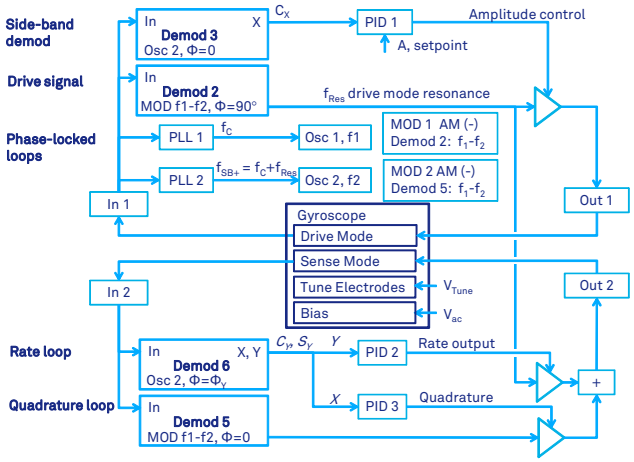

Figure 10. Gyroscope control with both closed-loop drive-mode and force-to-rebalance (FTR), when the carrier modulation is employed.

The schematic in Figure 10 assumes that there is a 90 degree phase shift between the applied force and the displacement at resonance, i.e. phase of the modulator output in Demodulator 2 is set to 90 degrees. In the case when the gyroscope's front-end electronics adversely affects this phase relationship, the schematic in Figure 11 can be implemented. As opposed to AC quadrature nulling as proposed in Figure 10, the quadrature correction can be accomplished by applying DC voltage to the dedicated gyroscope electrodes. Instead of feeding back a dynamic signal via the Output 2 (see Figure 10), the output from PID 3 is fed back to quadrature tuning electrodes via the auxiliary output Aux 1.This frees up the modulator output of Demodulator 2, which can be set to an arbitrary drive phase Φ_X, at which the amplitude is maximum. The modulator output of Demodulator 5 with modulation phase of 90 degrees is now used for nulling the rate signal.

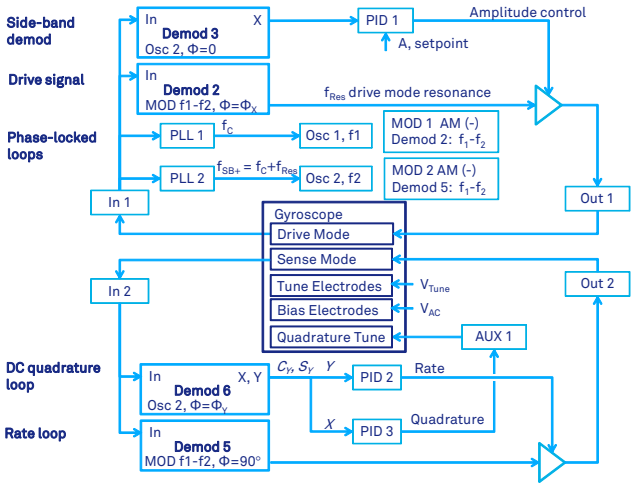

Figure 11. Gyroscope control with force-to-rebalance, carrier modulation and DC quadrature tuning.

Whole-angle readout

As opposed to the rate measuring mode with the predetermined axis of vibrations, the angle measuring mode (whole-angle) requires free precession of the vibration pattern. The whole-angle readout is also a way to operate a gyroscope without errors induced by a drive force. The whole-angle readout shown in Figure 11 was implemented to obtain the result in (Prikhodko 2011) and (Prikhodko 2013). As shown in Chapter 5 in (Prikhodko 2013), the demodulated components c_x, s_x, c_y, s_y (Equation 7 and Equation 8) of the gyroscope's pick-off signals are used to compute the quadratic invariants and from this the instantaneous value of the precession angle Θ(t) (Lynch 1998). In (Prikhodko 2011), the whole-angle operation was employed in open loop. To initiate vibrations, the gyroscope with 2 kHz operational frequency was electrostatically driven into the anti-phase resonant motion using a phase-locked loop, which was then abruptly turned off (indicated by the init switch in Figure 12). An EAM technique with sideband demodulation was used to detect the oscillations of drive and sense modes and measure the precession angle. The angle is computed from demodulated components c_x, s_x, c_y, s_y offline by means of a computer.

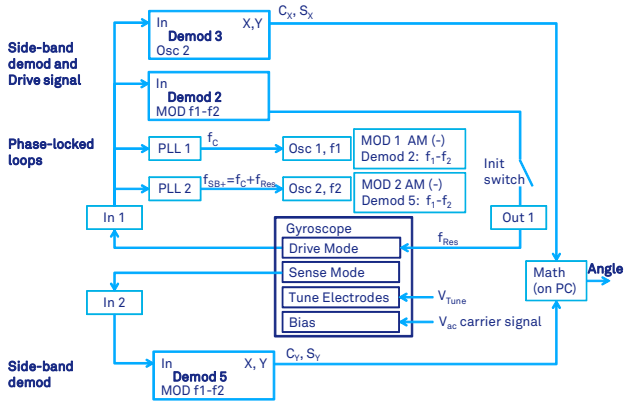

Figure 12. Gyroscope with carrier modulation in whole-angle mode with open loop readout.

Benefits for the HF2LI User

The control of vibratory gyroscopes is complex as multiple control loops need to run in parallel. Furthermore, high precision and low noise electronics are required throughout the setup to achieve maximum performance. The HF2LI Lock-in Amplifier is particularly well suited for gyroscope control, as it combines the required precision and flexibility in a single housing. Two low-noise inputs, six dual-phase lock-in amplifiers, two PLLs, four general purpose PID controllers and two signal generators are available and can be combined to provide the required functionality.

One single HF2LI device contains the features to control drive and sense mode vibrations with PLLs locked to the natural resonator frequency, force-to-rebalance control, quadrature control loop and carrier modulation techniques for optimal performance. This makes the HF2LI the most accurate commercially available lock-in amplifier in terms of separating quadrature component from useful in-phase component (representing Coriolis response in CVG).

Additional to the features mentioned above, the HF2LI provides a set of tools, which are not mentioned before in this paper, but which greatly help the experimenter to analyze the measurement setup and find the right parameters faster. They are all available in the standard user interface software.

- ZoomFFT: frequency spectrum around the resonance frequency. PLL stability and disturbances in the system, such as ground issues, can be debugged here
- PLL Advisor: simulator to find PLL parameters
- PID Tuner: simulator to find PID parameters
- Oscilloscope: shows the raw input and output signal
- Sweeper: helps to find the resonance frequency and the necessary phase shift to set the PLL on the resonance
- Spectroscope: provides the transient view of the frequency and amplitude signal. Helps to set the PID parameters and keep an eye on the device during the measurement
- Q-factor measurement by means of frequency sweeping or measurement of decay time (see blog on Q-factor measurement on www.zhinst.com)

Besides the HF2LI, Zurich Instruments also offers the UHFLI lock-in amplifier. The UHFLI can be operated at frequencies up to 600 MHz and comprises a very similar feature set to the HF2LI. The UHFLI has a lower minimum time constant and faster PID controllers. It is therefore suited for applications, which require a higher control bandwidth.

For further information and support on how to apply the HF2LI or UHFLI lock-in amplifiers to your specific gyroscope setup please contact Zurich Instruments.

Acknowledgements

This application note was written together with Igor Prikhodko, former member of the MicroSystems Laboratory of the University of California Irvine, now at Analog Devices, Inc., Wilmington, MA, USA.

We also would like to thank A. A. Trusov, A. M. Shkel, and S. A. Zotov from the MicroSystems Laboratory of the University of California Irvine for their insightful discussions regarding CVG and support.

References

[1] J. Bernstein et al. 1993. "A micromachined comb-drive tuning fork rate gyroscope," Proc IEEE Micro Electro Mechanical Systems Workshop (MEMS '93), Fort Lauderdale, pp. 143-148.

[2] J. A. Gregory, J. Y. Cho, “Novel Mismatch Compensation Methods for Rate-Integrating Gyroscopes”, In Proc: Position, Location, and Navigation Symposium (IEEE/ION PLANS 2012), Myrtle Beach, SC, USA, 23 Apr - 26 Apr 2012, pp. 252-258.

[3] P. Greiff, B. Boxenhorn, T. King, L. Niles, "Silicon monolithic micromechanical gyroscope", Solid-State Sensors and Actuators, 1991. Digest of Technical Papers, TRANSDUCERS '91, pp.966-968, 24-27 Jun 1991.

[4] HF2 User Manual, Zurich Instruments AG, Zurich, Switzerland, www.zhinst.com.
[5] R. P. Leland, “Mechanical-thermal noise in MEMS gyroscopes,” Sensors Journal, IEEE, 5(3), pp. 493-500, 2005.
[6] D. Lynch, “Coriolis Vibratory Gyros,” in Proc. of Symposium Gyro Technology, Stuttgart, Germany, 1998, pp. 1.0–1.14. (Reproduced as Annex B, Coriolis Vibratory Gyros, pp. 56–66 of IEEE Std. 1431–2004. IEEE Standard Specification Format Guide and Test Procedure of Coriolis Vibratory Gyros, IEEE Aerospace and Electronic Systems Society, 20 December, 2004.).
[7] I. P. Prikhodko, S. Zotov, A. Trusov, and A. Shkel, “Foucault pendulum on a chip: Angle measuring silicon MEMS gyroscope,” in Proc. of IEEE Micro Electro Mechanical Systems Conference (MEMS 2011), Cancun, Mexico, Jan. 23–27, 2011, pp. 161–164.
[8] I. P. Prikhodko, A. Trusov, and A. Shkel, “North-finding with 0.004 radian precision using a silicon MEMS quadruple mass gyroscope with Q-factor of 1 million,” in Proc. of IEEE Micro Electro Mechanical Systems Conference (MEMS 2012), Paris, France, Jan. 29–Feb. 2, 2012, pp. 164–167.
[9] I. P. Prikhodko, “Development of a Self-Calibrated MEMS Gyrocompass for North-Finding and Tracking”, Dissertation, University of California Irvine, 2013.
[10] I.P. Prikhodko, J.A. Gregory, C. Merritt, J.A. Geen, J. Chang, J. Bergeron, W. Clark, M.W. Judy, “In-Run Bias Self-Calibration for Low-Cost MEMS Vibratory Gyroscopes”, In Proc: Position, Location, and Navigation Symposium (IEEE/IONPLANS 2014), Monterey, CA, USA, 5 - 8 May 2014.
[11] A.M. Shkel, “Type I and Type II micromachined vibratory gyroscopes”, In Proc: Position, Location, and Navigation Symposium (IEEE/ION PLANS 2006), San Diego, CA, USA, 25–27 Apr. 2006, pp. 586–593.
[12] A. Trusov and A. Shkel, “A novel capacitive detection scheme with inherent self-calibration,” IEEE/ASME Journal of Micro electromechanical Systems, vol. 16, no. 6, pp. 1324–1333, Dec. 2007.
[13] A. Trusov et al. “Force Rebalance, Whole Angle, and Self-Calibration Mechanization of Silicon MEMS Quad Mass Gyro,” IEEE International Symposium on Inertial Sensors and Systems (IEEE ISISS 2014), Laguna Beach, CA, USA, Feb. 25-26, 2014.
[14] J.-K. Woo, J. Y. Cho, C. Boyd, and K. Najafi, “Whole-Angle-Mode Micromachined Fused-Silica Birdbath Resonator Gyroscope (WA-BRG),” in Proc. of IEEE Micro Electro Mechanical Systems Conference (MEMS 2014), San Francisco, CA, USA, Jan. 26-30, 2014, pp. 20-23.
[15] H. Xie and G.K. Fedder, “Integrated MEMS Gyroscopes", Journal of Aerospace Engineering, Vol. 16 (2003), No. 2, p. 65-75.
[16] N. Yazdi, F. Ayazi, K. Najafi, "Micromachined inertial sensors," Proceedings of the IEEE, vol.86, no.8, pp.1640-1659, Aug 1998.

Zurich Instruments

Zurich Instruments
Technoparkstrasse 1
CH-8005 Zurich
Switzerland

Phone +41-44-5150410
Email info@zhinst.com
Web www.zhinst.com

About Zurich Instruments
Zurich Instruments makes lock-in amplifiers, phase-locked loops, and impedance spectroscopes that have revolutionized instrumentation in the high-frequency (HF) and ultra-high-frequency (UHF) ranges by combining frequency-domain tools and time-domain tools within each product. This reduces the complexity of laboratory setups, removes sources of problems and provides new measurement approaches that support the progress of research.